

Published in final edited form as:

Head Neck. 2012 November ; 34(11): 1640–1647. doi:10.1002/hed.21981.

Volumetric change of human papillomavirus–related neck lymph nodes before, during, and shortly after intensity-modulated radiation therapy

Giuseppe Sanguineti, MD^{1,*}, Francesco Ricchetti, MD¹, Binbin Wu, PhD¹, Nishant Agrawal, MD², Christine Gourin, MD², Harold Agbahiwe, MD¹, Shanthi Marur, MD³, Stefania Clemente, PhD¹, Todd McNutt, PhD¹, and Arlene Forastiere, MD³

¹Department of Radiation Oncology and Molecular Radiation Sciences, Johns Hopkins University, Baltimore, Maryland ²Department of Head and Neck Surgery, Johns Hopkins University, Baltimore, Maryland ³Department of Oncology, Johns Hopkins University, Baltimore, Maryland

Abstract

Background—To assess volumetric changes of human papillomavirus (HPV)-related lymph nodes (LN) before, during, and after a course of intensity-modulated radiation therapy (IMRT) ± chemotherapy.

Methods—Each “pathologic” LN (> 1 cm) was contoured on the available diagnostic/planning CTs before, during each week, and after treatment.

Results—Seventy-nine LNs in 50 patients were identified. Beyond the first week of treatment, 3 patterns of LN change were recorded: consistently shrinking LN ($n = 33$; 41.8%), inconsistently shrinking LN with temporary enlargement limited to the first week ($n = 14$; 17.7%), or also during the subsequent weeks ($n = 32$; 40.5%). Nodal density at planning is highly predictive of group assignment, with a larger mean density for consistently over inconsistently shrinking LNs ($p = .009$). Also, this grouping predicts the response at the end of treatment.

Conclusion—HPV-related LN behavior during IMRT is extremely variable but somewhat predictable on the basis of nodal density at planning.

Keywords

volumetric change; lymph nodes; IMRT

Compared to the classic tobacco and alcohol-related oropharyngeal squamous cell carcinoma (SCC), the detection of human papillomavirus (HPV) integration within cancer cells by in situ hybridization confers a better prognosis and a more favorable response to a variety of treatment strategies, including radiotherapy.¹⁻³ From a clinical perspective, one common presentation of HPV-related oropharyngeal SCC is represented by an early T classification (T1–2) tumor along with advanced nodal disease (N2–3).⁴ Nodal disease in HPV+ oropharyngeal SCC is often predominantly cystic on imaging,⁵ as opposed to solid or partially necrotic as in the case of other head and neck SCC.⁶

The extent and rate of volumetric change of lymph nodes (LNs) before, during and after intensity-modulated radiation therapy (IMRT) has potential implications on multiple aspects of treatment. A rapid response is associated with a favorable outcome.⁷⁻⁹ However, the extent and rate of regression during radiotherapy may influence the risk of complications, because the decreasing volume of the target may expose a higher-than-planned amount of normal tissue to a given dose.^{10,11} On the other hand, clinical observations before treatment suggest that cystic nodes often undergo sudden changes in volume⁵; similarly, it is not infrequent to observe a temporary enlargement of cystic nodes during a course of radiotherapy. Whether this phenomenon is real nodal enlargement rather than a relative increase compared to the “shrinkage” of the surrounding tissues due to dehydration and fasting is unclear because it has never been documented in a systematic way.

Finally, volumetric response measured a few weeks after the end of treatment is 1 important criterion to assess tumor response and decide whether further intervention, namely surgery, is necessary.¹² Unfortunately, cystic LNs tend also to be less fluorodeoxyglucose-avid than solid ones on pretreatment imaging, making morphologic criteria and particularly the absolute or percent regression the most important indicators of response.

There are no data in the literature on any of the above aspects of HPV-related nodal disease. In order to clarify some of them, we have undertaken the present study to describe the volumetric changes of previously untreated HPV-related nodal disease before, during, and shortly after IMRT.

MATERIALS AND METHODS

Patients and scans

Patients treated with definitive IMRT \pm chemotherapy for HPV-related SCC with disease metastatic to cervical LNs at Johns Hopkins University (JHU) undergo weekly Kilo-voltage (KV) CT scans in addition to the planning CT as part of an internal quality assurance (QA) program. The CT scan is tentatively acquired during each week of treatment based on the availability of the machine, without a fixed time interval between consecutive scans. For this particular study, we selected only those consecutive patients that fulfilled all 3 of the following criteria: (1) HPV (by in situ hybridization¹³)-related SCC treated at JHU between September 2007 and May 2010; (2) the presence of sizable “pathologic” adenopathy defined as at least 1 neck LN \geq 1 cm in largest diameter in levels IB to V (\geq 0.5 if retropharyngeal) on the planning CT; (3) no up-front treatment (neck dissection and/or induction chemotherapy). The purpose of the present study, which was approved by the local institutional review board, was to describe the volumetric change of each LN before, during, and shortly after treatment.

Lymph nodes

An LN was considered pathologic as defined above; if 2 or more nodal masses were matted or even just contiguous without a fat plane separating them, they were considered part of the same LN.

On each scan, each LN was retrospectively contoured as appropriate by a single observer (G. S.). An attempt was also made to try to contour the same LN on both the pretreatment and the posttreatment diagnostic CT scans, but this was dependent on the availability of the scan.

Within each patient, the nodal density at planning was computed as a percentage of the LN that showed a density below that of the sternocleidomastoid muscle,⁶ as detailed below. A representative portion of the sternocleidomastoid muscle was contoured on the planning CT

trying to avoid the surrounding fat or disease infiltration, if present (the contralateral sternocleidomastoid muscle was preferably chosen). Once contoured, its average density was extracted from Pinnacle³ (Philips, Madison, WI). Afterward, each previously contoured LN was isotropically shrunk by 1.5 mm to minimize inference from the surrounding structures or partial volume effects. Using an automated tool in Pinnacle,³ within each shrunken LN, we could identify and contour, slice by slice, the region that was below the density threshold provided by the sternocleidomastoid muscle. The resulting volume was divided by the overall volume of the shrunken LN and expressed as a percentage. Therefore, a value of 30% means that 30% of the volume of the shrunken LN shows a density below the density of the sternocleidomastoid muscle.

Intensity-modulated radiation therapy

All patients underwent a 3-level dose painting IMRT with the following total doses: 70 gray (Gy) to macroscopic disease (clinical target volume [CTV]1); 63 Gy to microscopic high-risk disease (CTV2); or 58.1 Gy to microscopic low-risk disease (CTV3), as previously reported.^{14,15} All doses were given for the same number ($n = 35$) of fractions over 7 weeks. Each CTV was expanded by 5 mm to the corresponding planning target volume.

Statistics

After each selected LN was contoured on the serial CT as appropriate, its volume was extracted from Pinnacle.³ All available image datasets were coregistered in Pinnacle³ before contouring. For each observation, we computed the absolute and the relative variation in volume compared to the one at planning.

LN doubling time before starting treatment was calculated using the volume of each available LN at both diagnosis and planning and the time elapsed between the 2 measurements as reported by others.^{16,17}

The absolute variation of each LN over time was plotted and fit to an exponential growth equation which provided the correlation coefficient and the halving time. We first assigned the computed value of relative change for each LN to a week of treatment based on the calendar day of IMRT delivery with respect to the first day of treatment (time = 0).¹⁸ Data computed from observations were recorded by week of treatment up to 7 weeks. For patients who had 2 observations during the same week of treatment, a mathematical average of the 2 was taken. No attempt was made to correct for missing data. Locally weighted scatter plot smoothing curves were used to illustrate the relative change of LNs across time in the groups. LNs were pooled into groups based on the pattern and the timing of relative changes during treatment: LNs that showed a consistent shrinkage at all observations (consistently shrinking LN [CS-LN]) were separated from those that enlarged at least once during treatment (inconsistently shrinking LN [IS-LN]). Moreover, within the latter group, we further divided LNs that enlarged only during the first week of treatment (IS1-LN) from those that grew also or only beyond the first week (group IS2/7-LN).

A complete nodal response after treatment was defined as either largest axial diameter <1 cm or 90% regression in volume on diagnostic CT. Regarding positron emission tomography (PET), LNs with a residual standardized uptake value less than 2 were defined as complete responders. Reassessment was typically done at 12 weeks after treatment completion.

Intraobserver variability was assessed for its impact on observed differences over LN volume as follows: LNs were recontoured by the same observer (G. S.) at least 2 months after the first pass, using the same procedure as outlined above, and blinded to the previous results. Intraobserver variability was estimated throughout the measurement error (ME; the

absolute difference between the 2 measured volumes of the same LN at the 2 readings) and the percentage ME (%ME; obtained by dividing the ME by the average of the 2 measurements for each LN).

Various statistical tests were used to compare different groups including the nonparametric Mann–Whitney *U* test, the Kruskal–Wallis test, and the Spearman’s rank correlation coefficient; distributions were tested with Pearson’s chi-square test; significance was claimed for *p* values < .05.

All analyses were performed using GraphPad (version 1.03, GraphPad Software, San Diego, CA) and PASW Statistics 18 (SPSS, Chicago, IL).

RESULTS

Patients and treatment

Fifty patients were selected for the present analysis. Main characteristics are reported in Table 1. All but 6 patients had primary oropharyngeal tumors. Median age was 57 years (range, 29–75 years). Most patients had early T classification (T1–2) and multiple nodes <6 cm (N2b–c). Median largest nodal axial diameter per patient was 2.75 cm (range, 1.1–6.5 cm). All but 1 patient received platinum-based concomitant chemotherapy. All patients completed IMRT as prescribed (to 70 Gy). Median overall treatment time was 7.0 weeks (range, 6.6–9.6 weeks).

Scans

Thirty-six patients (72%) had pretreatment diagnostic CT (dxCT) scans done at JHU and, therefore, available in Pinnacle³ for coregistration with the planning CT. The mean (SD) time interval between the dxCT and the planning CT was 5.3 (4.0) weeks.

All patients underwent a planning CT, which consists of a helical “lightly” contrast-enhanced CT (100 mL of Omnipaque 350 mg I/mL; GE Healthcare, Mississauga, Ontario; manually injected over 1–2 minutes), 3 mm slice thickness.

Moreover, 341 weekly CT scans were acquired during treatment. Weekly CT scans were identical to the planning CT, obtained on the same machine used for planning, with the exception of not being contrasted. Overall, a median number of 6 scans per patient were analyzed during treatment (range, 4–8 scans). The mean (SD) time interval between planning CT and the start of treatment was 2.3 (0.5) weeks.

All patients underwent a reevaluation CT ± PET after completion of treatment, except 1 patient who underwent a planned neck dissection without response assessment. The mean (SD) time between the imaging study and the end of treatment was 11.8 (2.4) weeks.

Overall, 476 CTs were contoured and analyzed.

Lymph nodes

At planning CT, 79 LNs were identified in 50 patients. Thirty-one patients had a single nodal mass which represented a conglomeration of matted nodes in 19. There were 12 patients with 2 LNs, 3 patients with 3 LNs, and 4 patients with 4 LNs. The number of contoured pathologic nodes per patient was limited to 4.

Mean LN volume at planning was 13 cc (SD, 16.8 cc) and mean (SD) LN dose at planning was extremely consistent at 72.6 (1.2) Gy.

The mean (SD) observed sternocleidomastoid muscle density across all 50 patients was 56 (6.3) HU. Based on the percentage of the hypodense part, individual nodal density ranged from 0 (completely solid) to 100% (completely cystic), with a median value of 29%.

There was no correlation between nodal volume and nodal density at planning (Spearman's $\rho = 0.15$; $p = .18$).

A pretreatment nodal fine needle aspiration (FNA) was performed in 29 patients (58%) of whom 17 patients had it performed before referral at JHU. Because the FNA could potentially affect nodal volume change, and it was often unclear which LN had undergone FNA, selected parts of the analysis were rerun only in patients who did not undergo an FNA (40 LNs, 21 patients).

Intraobserver variability

After categorization into 3 groups based on the tertile volume at planning, 9 LNs were randomly selected from each subgroup resulting in 27 recontours. Overall, the mean and median ME were 0.6 cc and 0.3 cc; in terms of %ME, these would correspond to 7.8% and 6.5%, respectively.

LNs smaller than 2.85 at planning had a larger mean %ME than bigger ones (12.4% vs 5.4%; $p = .003$). After correcting for volume size (9 small LNs were replaced by 9 larger nodes), LN density at planning did not affect intraobserver variability ($p = .9$).

Pretreatment lymph node doubling time

Results for the 59 available LNs (36 patients) are summarized in Table 2. Data were sorted from the fastest growing to the fastest shrinking LN.

In 17 of 59 LNs (28.8%), the pretreatment LN doubling-time was negative, consistent with a reduction in volume between the dxCT and the planning CT. The average (SD) absolute and relative shrinkage were 1.2 cc (1.4) and 20% (24%) of the volume at planning. There was a positive correlation between the volume at planning and pretreatment LN doubling-time ($\rho = 0.27$; $p = .042$) but not between nodal density and pretreatment LN doubling-time ($\rho = 0.07$; $p = .59$).

After excluding LN <2.85 cc and those potentially aspirated, still 27.7% of LN (5 of 18) decreased in volume between the 2 observations.

Pattern of volumetric change over baseline during intensity-modulated radiation therapy

Thirty-three LNs (41.8%) showed a consistent shrinkage over baseline (planning) with a progressive decrease in volume at any observation during treatment. The semi-logarithmic plot of the absolute volume over time for each of the 33 CS-LN is reported in Figure 1. Linear regression of the plot of each of the LNs produced a median correlation coefficient of 0.94 (range, 0.81–0.99). Median halving time was 17.6 days (range, 8.3–62.6 days).

The remaining 46 LNs (58.2%) were found to be enlarged at least once during IMRT compared to baseline or a previous observation during treatment (Figure 2).

In 14 LNs (17.7%), the enlargement was limited to the first week of treatment (IS1-LN) and by definition always exceeded the baseline volume; the recorded average peak increase was 110.9% (SD, 20.5%), exceeding 110% in 5 of 14 LNs (35.7%). When 6 nodes <2.85 cc at planning were excluded, the average (SD) percent change was 108.4% (8.5%); within this group, only in 1 of 8 LNs the maximum relative increase exceeded 115% with a peak at 126%. The median (range) halving time beyond the peak was 17.9 days (range, 8.2–27.4

days) and remarkably similar to the 1 of CS-LN ($p = .92$), as illustrated in Figure 3 and summarized in Table 3.

For the remaining 32 LNs (40.5%; group IS-LN-2/7), the enlargement was recorded after week 1 ($n = 29$) or during and beyond week 1 ($n = 3$). As shown in Table 3, the relatively large SD suggests high variability among LNs of this group. Of them, 8 LNs (10.1%) never exceeded the baseline volume that implies that they regressed to some extent before enlarging; conversely, 24 LNs (30.4%) exceeded the baseline volume with median/mean peak enlargements of 116% and 137%, respectively. As shown in Figure 4, the peak prevalence of observations exceeding 125% and 150% was 30.4% and 13%, respectively, at week 3. Moreover, the mean number of weeks with observations exceeding 100% is 3.2 (SD, 1.9) per LN with 80% of LNs enlarged for more than 1 week. The average dropped from 3.2 to 1.3 (2.2) when only observations exceeding 125% were selected.

For IS2/7-LNs, the median halving time beyond the peak was 25.6 days (range, 5.2–230 days) and significantly longer than the 1 of CS-LN and IS1-LN combined ($p = .045$).

LN behavior was correlated in patients: of 12 patients with 2 LNs, 10 (83.3%) had LNs belonging to the same group; Spearman's correlation coefficient was 0.74 ($p = .006$).

Predictors of group assignment

Average nodal volume at planning was not statistically different among the 3 groups; moreover, the average time from simulation to treatment start was similar in all groups.

Mean density at planning was larger for CS-LNs (24.9%; SD 23.5%) than IS-LNs (46.2%; SD 34.4%; $p = .009$). Moreover, IS2/7-LNs showed a significantly lower average density (53.3%; SD, 33.2%) than both IS1-LNs (30.1%; SD, 32.6%; $p = .038$) and CS-LNs ($p = .001$). There was no difference in density at planning between CS-LN and IS1-LN ($p = .97$).

Nodal density was further categorized into 3 groups based on tertiles. In the majority of cases (85%), a solid LN decreased in size rapidly (group CS or IS1). Conversely, when the cystic component within the LN was >19%, the probability of enlargement during weeks 2 to 7 of treatment was about 50% (Table 4). A receiver operating characteristic analysis was done in order to explore further the optimal cutoff value of LN density for group IS2/7-LN assignment. The result was 21.5% (sensitivity, 87.5%; specificity, 57.4%; area under curve, 0.733; 95% confidence interval, 0.616–0.850; $p < .001$), close to the previously used lower tertile.

The results hold for LNs that did not undergo pretreatment FNA.

LNs that had a negative pretreatment doubling-time were equally distributed among groups ($p = .76$).

Response at reevaluation

Of 75 assessed LNs, 19 (25.3%) failed to show a complete response at CT on reevaluation. Density ($p = .031$) and volume at planning ($p < .0001$) were correlated to the probability of observing a (morphologic) clinical complete response after treatment. As shown in Table 5, LNs belonging to group IS2/7 were less likely to respond completely on CT ($p = .019$), PET ($p = .073$), and more likely underwent neck dissection ($p = .042$). However, at a median follow-up of 24.8 months (range, 13–38.6 months), both the distribution of persistent tumors cells in the dissected specimen and the number of regional failures were not distributed differently among groups. Of note, within the group of IS2/7-LN, we observed 1 case in which the pathology specimen showed persistent viable tumor cell despite a negative PET.

DISCUSSION

This study documents the atypical behavior of HPV-related LNs before (spontaneous shrinkage), during (enlargement), and shortly after (poor response) IMRT. Overall, these data bring new insights on the natural history of this disease and have implications on several aspects of its management, including staging, radiotherapy delivery, and response evaluation.

Two studies have investigated the pretreatment doubling-time of various head and neck SCC by considering the primary \pm nodal tumor volume change during the waiting time for radiotherapy.^{16,17} HPV status of the tumors was not provided. According to Jensen et al,¹⁶ the quartile of patients with the highest growth rates had a median doubling time of 27 days (range, 15–35 days) and for the half of patients with the fastest growing tumors it was 30 days (range, 15–99 days). In contrast, we found values of 69 days (range, 24–93 days) and 93 days (range, 24–402 days), respectively (Table 2). Overall, the median doubling time of our series (408 days) was significantly longer than the doubling time reported by Jensen et al¹⁶ (99 days) and Waaijer et al¹⁷ (57 days) and may be related to HPV infection. Studies focusing on the comparative analysis of cell kinetics in both HPV-positive and negative head and neck SCC have produced controversial results.^{19,20} It is also possible that the longer median doubling time found in the present study simply reflects the presence of a negative pretreatment doubling time in almost 30% of LNs. Interestingly, results were not affected by a previous nodal manipulation (FNA) and the amount of observed change was, on average, twice the ME, suggesting that it cannot be entirely explained by intraobserver variation in contouring. Why some HPV-related LNs shrink spontaneously is unclear; it has been hypothesized to be related to fluctuations in their cystic component,⁵ although we did not find a correlation between the nodal density at planning and shrinkage. The documented fluctuations in nodal volume before treatment have implications on nodal size questioning both the reliability and consistency of pretreatment clinical staging. Moreover, our data suggest that the volume at planning may overestimate the nodal volume at treatment in up to 30% of LNs.

After the first week of treatment, we found that more than half of LNs shows a progressive shrinkage with averages halving time of approximately 17 to 18 days and shrinkage to approximately 20% of the baseline volume toward the end of treatment. With the caveat that this represents the fastest regressing group of LNs, our results are consistent with literature data.^{8,21,22}

From an “adaptive” viewpoint, it has been shown that the tissue loss from tumor regression and/or weight loss during treatment can lead to increased dose to several critical structures^{10,23} and, in particular, the regression of LNs abutting the parotids can increase the dose to the glands.¹¹ The dosimetric implications are specific to a given anatomic/dosimetric configuration and difficult to predict because these are dependent on multiple factors including the location of the LN, its initial volume and shape, the extent and duration of regression, the deformation of surrounding tissues (weight loss), and the geometry of irradiation. However, it is intriguing that the mean LN volume reported in the current study (13 cc; SD, 16.8) is close to the mean initial volume (17.8 cc) of the LNs in the study of Kuo et al,¹¹ where a statistical lower dose to the parotid gland was achieved after replanning at 45+ Gy.

The present study differentiated between LN enlarged (only) during week 1, as expression of a continuous growth during radiotherapy waiting time, from those found to be enlarged over baseline (also) in the subsequent weeks of treatment. The latter pattern was observed in about 30% (24 of 79) of LNs and, to our knowledge, has not been described before.

Moreover, we found that solid LNs rarely (2 of 24; 8.3%) show this behavior, suggesting that this is probably related to cystic components. Two features are potentially worrisome for proper radiotherapy delivery: the amount of enlargement and its duration. In Figure 5, we illustrate the case of an LN that increased in volume by about 2/3 (from 60.6 cc to 98.9 cc) from planning to week 5. As a reference, if the node were spherical, this would correspond to an absolute average increase in diameter of approximately 7 mm and thus potentially relevant from a dosimetric standpoint. If the node were ellipsoid, the change along the larger axis would have been even larger.

We also document the lack of a morphologic complete response in a significant proportion of IS2/7-LN at reevaluation after treatment. The fact that bulky and/or necrotic LNs from various head and neck SCC take longer to respond and/or respond less favorably to treatment has been known for decades.^{6,7} However, in the current study, cystic nodes are constituted mostly by fluid and likely to contain fewer cancer cells (usually confined to the thin walls)⁵ compared to their solid/necrotic counterparts. Therefore, it is unclear whether the slower response should be considered a poor predictor of outcome or not.⁹ The present (preliminary) data (Table 5) failed to show a detrimental effect of nodal group on regional control, although the limited number of events prevents firm conclusions. However, the present analysis clearly shows that the cystic node represents a challenge at reevaluation, because it is less likely to respond on CT and PET may not be reliable in this setting due to the poor fluorodeoxy-glucose avidity of the cystic component. The use of functional imaging that is able to detect “viable” tumor cells after treatment²⁴ has not been tested in this particular setting.^{25,26} We report 1 case in which residual viable tumor cells were found despite a negative reassessment PET (Table 5). This uncertainty is reflected in our practice where the number of dissected IS2/7-LNs approached the number of LNs without a complete morphological response. Moreover, the fact that 3 of 12 (25%) IS2/7-LNs that did not respond completely at CT, were found to contain residual viable tumor cells at pathology supports this approach.

We acknowledge that the present analysis has limitations, as discussed elsewhere.¹⁸ Even if not all LNs had observations at each time point, overall, we collected 287 of 350 (82%) observations during treatment, that is remarkable. The first week is the one with the largest number of missing observations (28% of LNs). As a result, we acknowledge that the number of patients with temporary enlarged nodes during the first week may have been slightly underestimated, although this has likely very limited impact on both the group assignment and the estimate of changes beyond week 1. Contours were drawn by a single observer on high quality KVCT scans resulting in a low ME. The median %ME of 6.5% of the present study compares favorably to the value of 7% reported by others.²⁷

In conclusion, this article documents the unexpected behavior of HPV-related LNs before and during IMRT. Some of these aspects are somewhat predictable on the basis of the nodal density at planning. Future studies will need to check the predictive value of pretreatment nodal staging on outcome; also, more data focusing on cystic nodes are needed to assess the role of posttreatment imaging on response. Regarding changes observed during IMRT, it would be reasonable to assess the volumetric enlargement (and its dosimetric consequences) of cystic nodes from the second week of treatment and from the fourth to fifth week if solid and bulky.

References

1. Ang KK, Harris J, Wheeler R, et al. Human papillomavirus and survival of patients with oropharyngeal cancer. *N Engl J Med*. 2010; 363:24–35. [PubMed: 20530316]

2. Fakhry C, Westra WH, Li S, et al. Improved survival of patients with human papillomavirus-positive head and neck squamous cell carcinoma in a prospective clinical trial. *J Natl Cancer Inst.* 2008; 100:261–269. [PubMed: 18270337]
3. Rischin D, Young RJ, Fisher R, et al. Prognostic significance of p16INK4A and human papillomavirus in patients with oropharyngeal cancer treated on TROG 02.02 phase III trial. *J Clin Oncol.* 2010; 28:4142–4148. [PubMed: 20697079]
4. Gillison ML. Human papillomavirus and prognosis of oropharyngeal squamous cell carcinoma: implications for clinical research in head and neck cancers. *J Clin Oncol.* 2006; 24:5623–5625. [PubMed: 17179099]
5. Goldenberg D, Begum S, Westra WH, et al. Cystic lymph node metastasis in patients with head and neck cancer: an HPV-associated phenomenon. *Head Neck.* 2008; 30:898–903. [PubMed: 18383529]
6. Munck JN, Cvitkovic E, Piekarski JD, et al. Computed tomographic density of metastatic lymph nodes as a treatment-related prognostic factor in advanced head and neck cancer. *J Natl Cancer Inst.* 1991; 83:569–575. [PubMed: 1848639]
7. Bataini JP, Bernier J, Asselain B, et al. Primary radiotherapy of squamous cell carcinoma of the oropharynx and pharyngolarynx: tentative multivariate modelling system to predict the radiocurability of neck nodes. *Int J Radiat Oncol Biol Phys.* 1988; 14:635–642. [PubMed: 3350718]
8. Bartelink H. Prognostic value of the regression rate of neck node metastases during radiotherapy. *Int J Radiat Oncol Biol Phys.* 1983; 9:993–996. [PubMed: 6408042]
9. Yang SN, Liao CY, Chen SW, et al. Clinical implications of the tumor volume reduction rate in head-and-neck cancer during definitive intensity-modulated radiotherapy for organ preservation. *Int J Radiat Oncol Biol Phys.* 2011; 79:1096–1103. [PubMed: 20605362]
10. Hansen EK, Bucci MK, Quivey JM, Weinberg V, Xia P. Repeat CT imaging and replanning during the course of IMRT for head-and-neck cancer. *Int J Radiat Oncol Biol Phys.* 2006; 64:355–362. [PubMed: 16256277]
11. Kuo YC, Wu TH, Chung TS, et al. Effect of regression of enlarged neck lymph nodes on radiation doses received by parotid glands during intensity-modulated radiotherapy for head and neck cancer. *Am J Clin Oncol.* 2006; 29:600–605. [PubMed: 17148998]
12. Ojiri H, Mendenhall WM, Stringer SP, Johnson PL, Mancuso AA. Post-RT CT results as a predictive model for the necessity of planned post-RT neck dissection in patients with cervical metastatic disease from squamous cell carcinoma. *Int J Radiat Oncol Biol Phys.* 2002; 52:420–428. [PubMed: 11872288]
13. Westra WH. The changing face of head and neck cancer in the 21st century: the impact of HPV on the epidemiology and pathology of oral cancer. *Head Neck Pathol.* 2009; 3:78–81. [PubMed: 20596995]
14. Sanguineti G, Adapala P, Endres EJ, et al. Dosimetric predictors of laryngeal edema. *Int J Radiat Oncol Biol Phys.* 2007; 68:741–749. [PubMed: 17398024]
15. Sanguineti G, Gunn GB, Endres EJ, Chaljub G, Cheruvu P, Parker B. Patterns of locoregional failure after exclusive IMRT for oropharyngeal carcinoma. *Int J Radiat Oncol Biol Phys.* 2008; 72:737–746. [PubMed: 18486356]
16. Jensen AR, Nellemann HM, Overgaard J. Tumor progression in waiting time for radiotherapy in head and neck cancer. *Radiother Oncol.* 2007; 84:5–10. [PubMed: 17493700]
17. Waaijer A, Terhaard CH, Dehnad H, Hordijk GJ, van Leeuwen MS. Tumor growth during the waiting period for radiotherapy in patients with oropharyngeal carcinoma. *Ned Tijdschr Geneeskd.* 2003; 147:1277–1282. Article in Dutch. [PubMed: 12861670]
18. Ricchetti F, Wu BB, McNutt T, et al. Volumetric change of selected organs at risk during IMRT for oropharyngeal cancer. *Int J Radiat Oncol Biol Phys.* 2011; 80:161–168. [PubMed: 21306971]
19. Hafkamp HC, Mooren JJ, Claessen SM, et al. P21 Cip1/WAF1 expression is strongly associated with HPV-positive tonsillar carcinoma and a favorable prognosis. *Mod Pathol.* 2009; 22:686–698. [PubMed: 19305381]
20. Rittà M, De Andrea M, Mondini M, et al. Cell cycle and viral and immunologic profiles of head and neck squamous cell carcinoma as predictable variables of tumor progression. *Head Neck.* 2009; 31:318–327. [PubMed: 19072995]

21. Barker JL Jr, Garden AS, Ang KK, et al. Quantification of volumetric and geometric changes occurring during fractionated radiotherapy for head-and-neck cancer using an integrated CT/linear accelerator system. *Int J Radiat Oncol Biol Phys.* 2004; 59:960–970. [PubMed: 15234029]
22. Bessell EM, Catterall M. The regression of tumors of the head and neck treated with neutrons. *Int J Radiat Oncol Biol Phys.* 1983; 9:799–807. [PubMed: 6305891]
23. Castadot P, Lee JA, Geets X, Grégoire V. Adaptive radiotherapy of head and neck cancer. *Semin Radiat Oncol.* 2010; 20:84–93. [PubMed: 20219546]
24. Pellitteri PK, Ferlito A, Rinaldo A, et al. Planned neck dissection following chemoradiotherapy for advanced head and neck cancer: is it necessary for all? *Head Neck.* 2006; 28:166–175. [PubMed: 16240327]
25. Porceddu SV, Pryor DI, Burmeister E, et al. Results of a prospective study of positron emission tomography-directed management of residual nodal abnormalities in node-positive head and neck cancer after definitive radiotherapy with or without systemic therapy. *Head Neck.* 2011 Epub ahead of print.
26. Moeller BJ, Rana V, Cannon BA, et al. Prospective risk-adjusted [18F]fluorodeoxyglucose positron emission tomography and computed tomography assessment of radiation response in head and neck cancer. *J Clin Oncol.* 2009; 27:2509–2515. [PubMed: 19332725]
27. Gordon AR, Loevner LA, Shukla–Dave A, et al. Intraobserver variability in the MR determination of tumor volume in squamous cell carcinoma of the pharynx. *AJNR Am J Neuroradiol.* 2004; 25:1092–1098. [PubMed: 15205156]

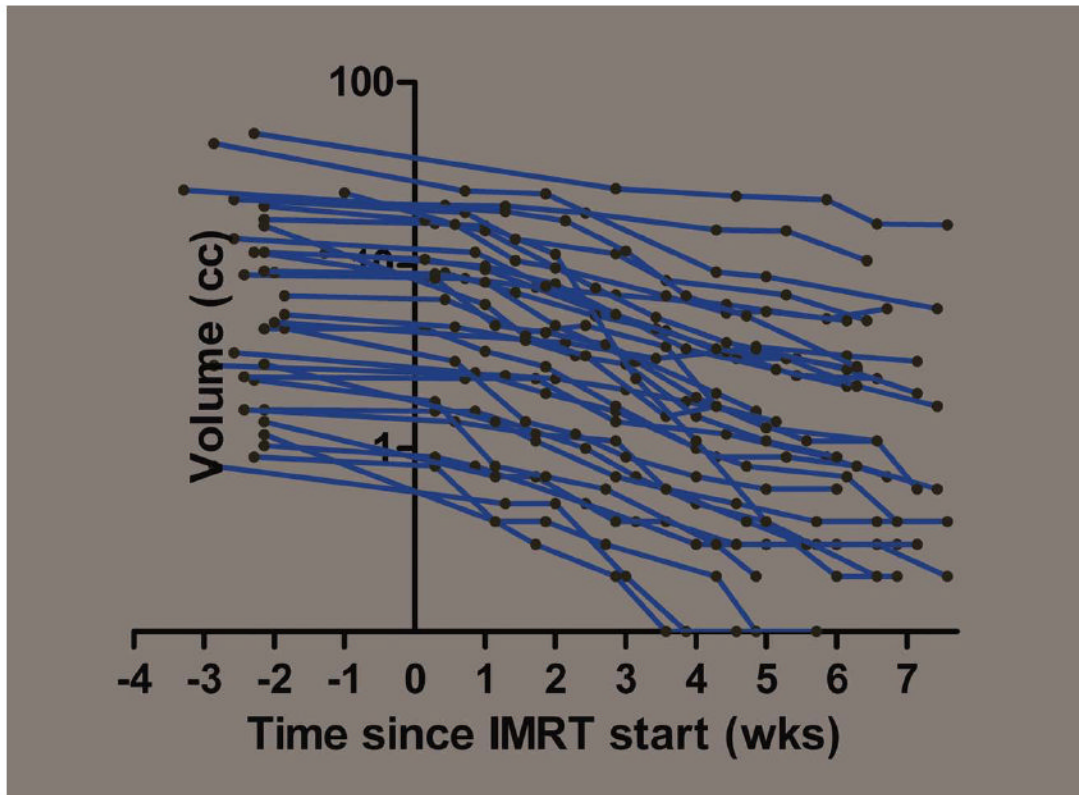


FIGURE 1. Semilogarithmic plot of the absolute volume of each individual lymph node (LN) which consistently shrunk at each observation during treatment ($n = 33$). [Color figure can be viewed in the online issue, which is available at wileyonlinelibrary.com.]

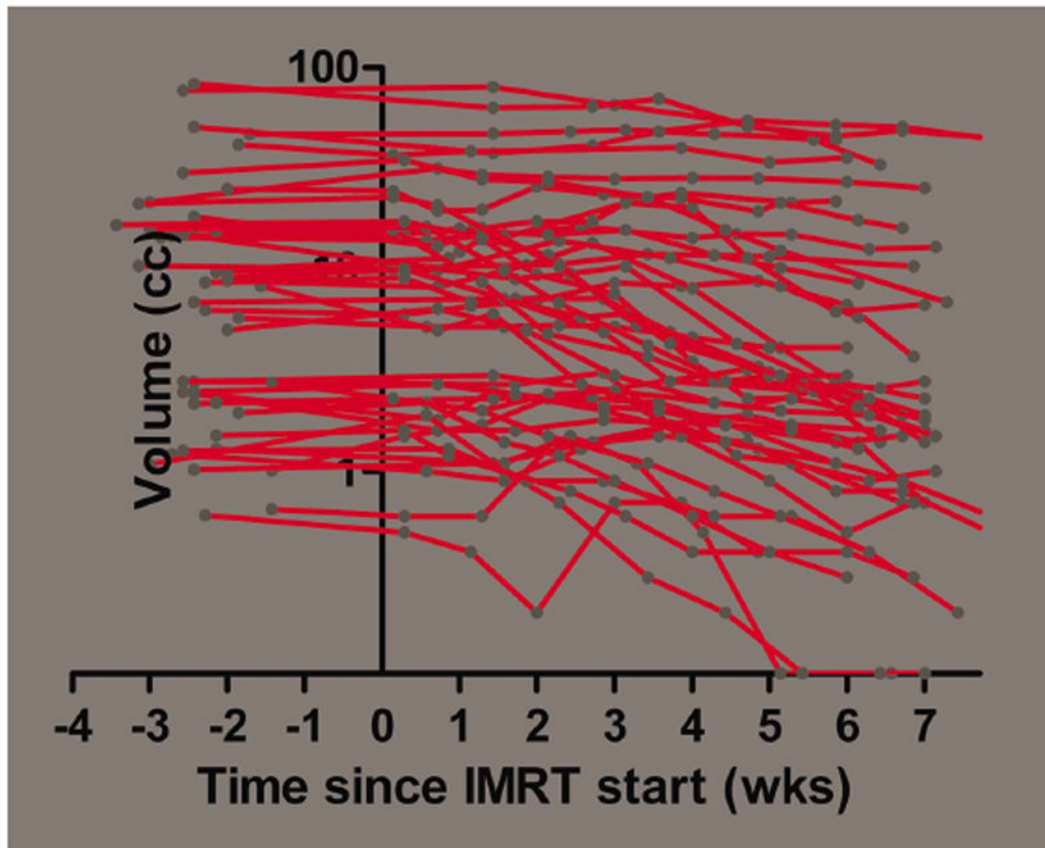


FIGURE 2.

Semilogarithmic plot of the absolute volume of each individual lymph node (LN) which did not shrink consistently during intensity-modulated radiation therapy (IMRT; $n = 46$). [Color figure can be viewed in the online issue, which is available at wileyonlinelibrary.com.]

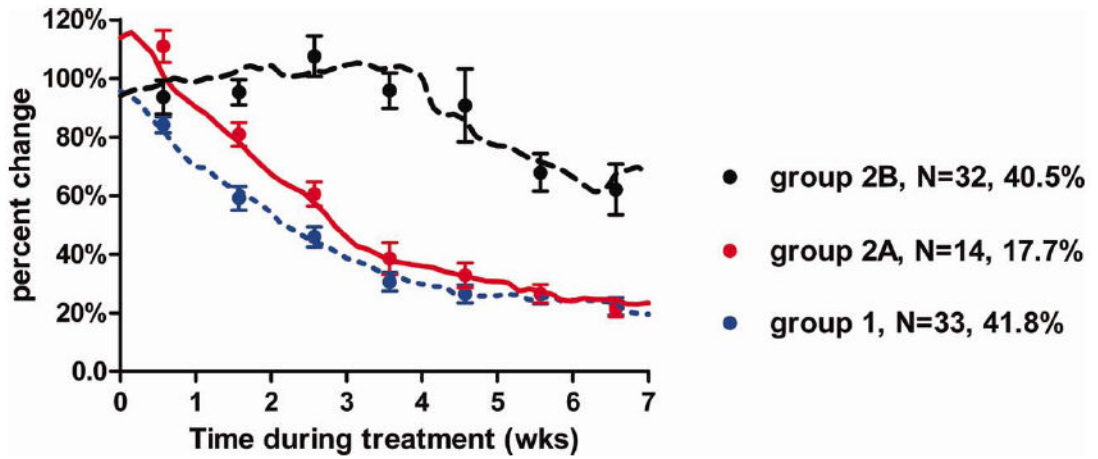


FIGURE 3.

Temporal relative change of volumes during treatment by group by locally weighted scatter plot smoothing (LOWESS) curves. Dots represent the averaged observations (with the standard error of the mean) computed for each week. [Color figure can be viewed in the online issue, which is available at wileyonlinelibrary.com.]

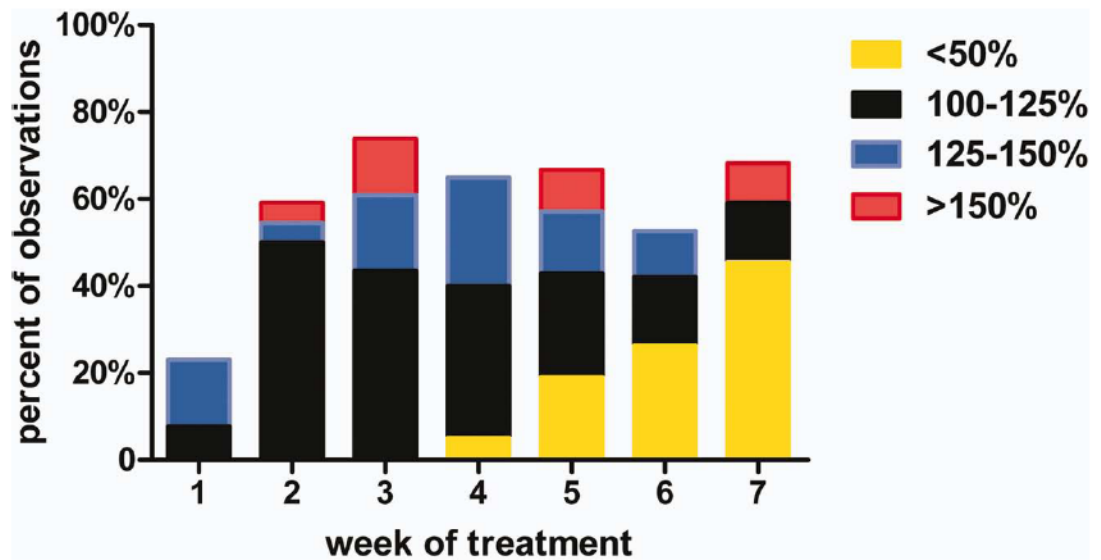


FIGURE 4. Distribution of observed relative changes from baseline for group IS2/7-lymph node (LN) by treatment week. [Color figure can be viewed in the online issue, which is available at wileyonlinelibrary.com.]

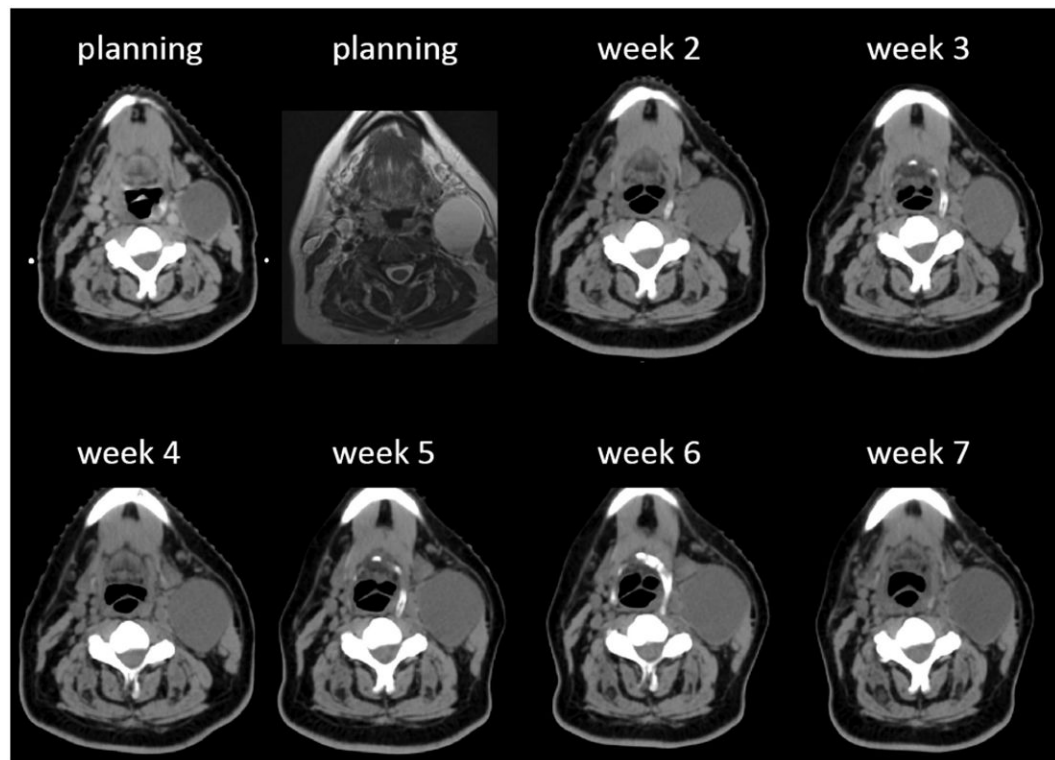


FIGURE 5. Planning/weekly CT scans and (T2W) MR images of a patient with a left level II to III cystic lymph node (LN). See text for explanation.

TABLE 1

Selected patient, tumor, and treatment characteristics.

Characteristic	No. of patients	%
Sex		
Male	46	92
Female	4	8
Primary tumor site		
Tonsil	19	38
Base of tongue	25	50
Unknown	3	6
Hypopharynx	1	2
Larynx	1	2
Nasopharynx	1	2
T classification		
T0	3	6
T1	15	30
T2	26	52
T3	4	8
T4	2	4
N classification		
N1	4	8
N2a	2	4
N2b	34	68
N2c	8	16
N3	2	4
HPV		
Positive	46	92
Negative (p16+)	4	8
FNA		
No	21	42
Yes	29	58
Chemotherapy		
CDDP	43	86
None	2	4
Other*	5	10

Abbreviations: HPV, human papillomavirus; FNA, fine-needle aspiration; CDDP, cis-diamminedichloroplatinum.

* 3, 1, 1 patients received concomitant carboplatin, erbitux or carboplatin + taxol, respectively.

TABLE 2

Pretreatment median (range) LN doubling time by quartile.

Time by quartile, d				
	First quartile	Second quartile	Third quartile	Fourth quartile
59 LNs	69 (24 ÷ 93)	153 (93 ÷ 402)	1041 (414 ÷ -6576)	-225 (-1386 ÷ -18)

Abbreviation: LN, lymph node.

TABLE 3

Mean (SD) percent change of LN during treatment by group

Group	No. of patients	Wk 1		Wk 2		Wk 3		Wk 4		Wk 5		Wk 6		Wk 7	
		Mean (%)	SD (%)	Mean (%)	SD (%)	Mean (%)	SD (%)	Mean (%)	SD (%)	Mean (%)	SD (%)	Mean (%)	SD (%)	Mean (%)	SD (%)
CS-LN	33	84.2	13.4	59.1	20.6	45.9	18.1	30.6	15.2	26.5	17.1	26.3	14.8	22.3	14.2
IS-LN	46	101.2	24.0	91.1	22.2	92.6	39.1	79.2	38.4	73.4	61.5	53.8	34.2	50.6	43.1
IS1	14	110.9	20.5	80.9	14.0	60.6	15.3	38.5	18.1	32.8	14.8	26.6	11.7	21.3	8.8
IS2-7	32	93.6	24.0	95.2	22.2	107.5	39.1	95.8	38.4	90.8	61.5	67.9	34.2	62.1	43.1

Abbreviations: LN, lymph node; CS-LN, consistently shrinking LN; IS-LN, inconsistently shrinking LN; IS1, inconsistently shrinking during the first week; IS2-7, inconsistently shrinking after the first week.

TABLE 4

Distribution of LN according to density at planning

Nodal density	Group			Overall
	CS-LN	IS1-LN	IS2-7-LN	
<19% (solid)	14	8	4	26
19-48% (int)	12	1	14	27
>48% (cystic)	7	5	14	26
Overall	33	14	32	79

Abbreviations: LN, lymph node; CS-LN, consistently shrinking LN; IS1-LN, inconsistently shrinking of lymph node during the first week; IS2-7-LN, inconsistently shrinking of lymph node after the first week.

See text for definition of density.

Pearson's chi-square p value is .008.

TABLE 5

Outcome of LN by group

	Overall	Incomplete responders		Dissected	Residual tumor on path	Overall regional fail ^{a*}
		CT	PET			
CS	33	6	0	1	0	1 [†]
IS1	14	1	1	1	0	0
IS2-7	28	12	4	9	3 [‡]	3
<i>p</i> value		.019	.073	.042	.35	.32

Abbreviations: LN, lymph node; PET, positron emission tomography; CS, consistently shrinking; IS1, inconsistently shrinking during the first week; IS2-7, inconsistently shrinking after the first week.

* Includes both clinical failure and the detection of viable tumor cells in the resected specimen.

[†] 1 patient failed after a complete clinical response at both CT and PET.

[‡] 1 patient had a negative PET.